International Journal of Pharmaceutical Science and Research
www.pharmacyjournal.net
ISSN: 2455-4685
Received: 03-05-2026, Accepted: 03-06-2026, Published: 18-06-2026
Volume 11, Issue 2, 2026, Page No. 78-85

Synthesis and evaluation *in vitro* anticancer activity of certain pyrazole based derivatives having potential inhibitors of cyclin dependent kinases (CDKs)

Mohammed Modhafer Filayyih[1], H N K AL-Salman[1], Mazin A A Najm[2]
[1] Department of Pharmaceutical Chemistry, College of Pharmacy, University of Basrah, Basrah, Iraq
[2] Department of Pharmacy, Mazaya University College, Iraq
DOI: https://doi.org/10.66856/ijpsr.2026.11.3.11037

Abstract
Background: Cancer is one of the most important global public health issues and although we have made significant progress in the diagnosis and treatment, it remains a serious challenge for modern medicine.
Aim: Rationally design and synthesize three thiourea derivatives (IVa–IVc) that may preserve the selective anticancer efficacy and relatively low toxicity of roscovitine and achieve enhanced pharmacokinetic properties.
Methodology: Target derivatives were sequentially synthesized, characterized by FT-IR, NMR and EI-MS, and tested for antiproliferative activity against MCF-7 cells by MTT assay, with IC_{50} values relatively to roscovitine.
Results: Potent antiproliferative activities were observed against MCF-7 breast cancer cells with a series of thiourea derivatives (IVa–IVc). IVa and IVb were the best inhibitors (78.13% vs 97.87% for rescovitine with an IC_{50} of 15.9 μM; 75.23% vs 97.87% for rescovitine with an IC_{50} of 15,9 μM) among the synthesized compounds while all derivatives synthesized were predicted to have a good drug-likeness according to Lipinski´s Rule of Five as well as high gastrointestinal absorption. The cytotoxic activity of derivatives correlated to substituents in structure–activity relationship analysis, confirming that both electron-donating and electron-withdrawing substituents were beneficial for biological efficacy.
Conclusion: VIa and VIb appeared as lead candidates with comparably high cytotoxicity to rescovitine. VIa, when substituted with fluorine, showed the most activity and useful structure–activity relationships were featured for obtaining further derivatives with greater potency.

Keywords: MCF-7 inhibition, thiourea derivatives, rescovitine, anticancer agents, kinase inhibitors

Introduction

Cancer will be one of the most challenging health problems around the world in the twenty-first century [1]. It includes a heterogeneous collection of disorders that are distinguished by uncontrolled cellular growth, surrounding tissue invasion and the potential for malignant cells to metastasize in distant organs [2, 3]. Pathological processes typically originate from an accumulation of genomic mutations and epigenetic alterations that disrupt key regulatory mechanisms and signaling pathways in cells [4, 5].

The global burden of cancer continues to grow at an alarming rate [6]. As can be seen in recent international cancer statistics, each year millions of new cases are diagnosed, and the disease continues to represent one of the top causes of death globally. Cancer obstinacy and mortality keeps on increasing universally, speaking to a noteworthy worldwide general wellbeing challenge [7, 8]. Global cancer data estimated 20 million incident cases and 9.7 million cancer deaths worldwide in 2022 [9, 10, 17]. This means that the world over, one in five people will suffer from cancer in their lifetime and one man (in 9) and one woman (in 12) dies of this disease[11]. Expectations are that the global cancer burden could increase significantly in coming decades, because of population growth as well as aging and greater exposure to cancer risk factors [12, 13]. Epidemiological projections suggest that the number of new cases of cancer per year may increase to around 35 million cases annually by 2050, a dramatic increase relative to current estimates [14, 15].

Lung cancer is still the most common cause of cancer death worldwide, and breast cancer is one of the commonest form of diagnosis globally [16]. Urea derivatives are extensively investigated due to their anticancer potential showing substantial cytotoxic activity against different cancer cell lines. They mainly exert antitumor functions through inhibition of cell growth, functioning as apoptosis inducers and interference with the metabolism pathways associated with the sustenance of cancer cells, resulting in death [17]. Similarly, a large number of thiourea derivatives with strong anticancer effects have been reported. They have been found to be able to inhibit a number of cancer cell lines and are thought to potentially overcome mechanisms of drug resistance [18, 19]. Also, thiourea-based molecules can target the expression of important molecules related to tumor initiation, cancer development and transformation processes regulating signaling transduction pathways associated with the production of proteins implicated in increased oncogenesis and suppressing angiogenesis process essential for tumor vascularization and expansion [20, 21]. These properties permit the structural redesign of compounds, which can enhance selectivity or be designed for particular types of cancers or drug delivery approach. Furthermore, many thiourea derivatives have good physicochemical properties such as acceptable absorption, distribution, metabolism and excretion (ADME) profiles potentially making those worthwhile candidates for continued drug development and clinical use [22].

Methodology

1. General

All of the beginning supplies and reagents for the synthesis have been purchased from Sigma Aldrich and Baoji Guokang Bio/Technology Co., Ltd. without any purification earlier than further utilize. Melting points were measured in a Stuart Scientific melting point apparatus. Reactions were monitored by analytical thin–layer chromatography (TLC) in hexane–ethyl acetate. The ^{1}HNMR & ^{13}CNMR spectra were recorded at (Department of Chemistry, College of Education for Pure Sciences, University of Basrah) using a Bruker spectrometer operating at 400 MHz (for 1H NMR spectrum) and 101 MHz (for 13C NMR spectrum). Centered chemical shifts (δ) are reported in parts per million (ppm) using tetramethylsilane (TMS) as the internal reference. All fourier-transform infrared (FT-IR) spectra were acquired by using a Thermo Scientific Nicolet spectrophotometer at University of Basrah. Mass spectra were obtained by electron ionization mass spectrometry (EI-MS), available at the Faculty of Chemistry, University of Tehran. The Regional Center for Mycology and Biotechnology performed biological evaluations (MCF-7).

2. Synthesis

2.1 General Method of Synthesis of compound (IIa-c) Derivatives

In two separated beakers, 0.1 mole of Methyl 4-(halogen) benzoate was dissolved in dry toluene (30 mL). At another beaker add NAH in paraffin into 10 mL of toluene to confirm the separation of NAH from paraffin wax. After gas evolution ceased, add to the mixture beaker the reaction mixture was stirred with 1 mL of acetonitrile for an additional 45 minutes this mixture is heated a range from room temperature to 80 ºC for 4-8 hours (Fig. 1) [23]. The purity of Pyrazole based derivative was examined using TLC, and the eluent system consisted of hexane and ethyl acetate (2:1).

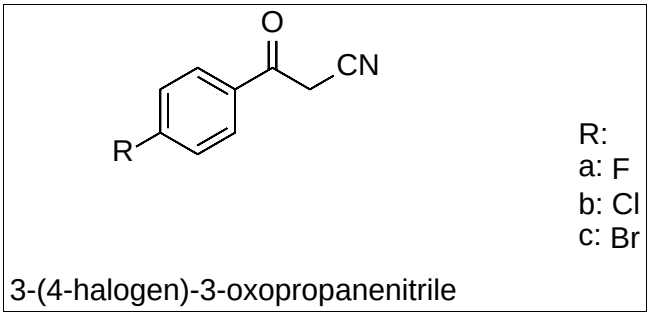

Fig 1: General structure of compound (IIa-c) and its derivatives

2.2 General Method of Synthesis of compound (IIIa-c) Derivatives

After synthesis of 3-(4-halogenphenyl)-3-oxopropanenitrile add 1 ml of Phenylhydrazine into the mixture and heated into 130 ºC for 15 minutes give Light yellow product of 1,3-bis(4-(halogen)phenyl)-1H-pyrazol-5-amine (Fig. 2). The purity of Pyrazole based derivative was examined using TLC, and the eluent system consisted of hexane and ethyl acetate (2:1) [24].

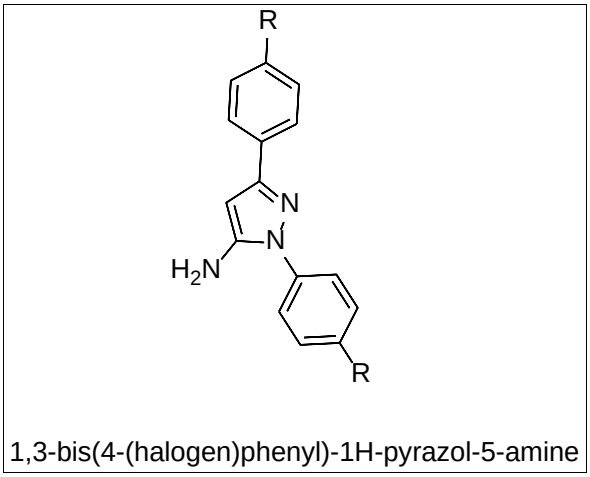

Fig 2: General structure of compound (IIIa-c) and its derivatives

2.3 General Method of Synthesis of compounds (IVa-e) Derivatives

Add glacial acetic acid (10 mL), and anhydrous sodium acetate (1.64 g) was added. The mixture was cooled to 0 °C, and chloroacetyl chloride (0.012 mol, 0.87 mL) was added drop wise with stirring. The reaction mixture was then refluxed for 1 hour at R.T and monitored by TLC monitoring (hexane /ethyl acetate 10:1) give reddish product after filtrated by water \ ethanol and by filter paper (Fig. 3) [25].

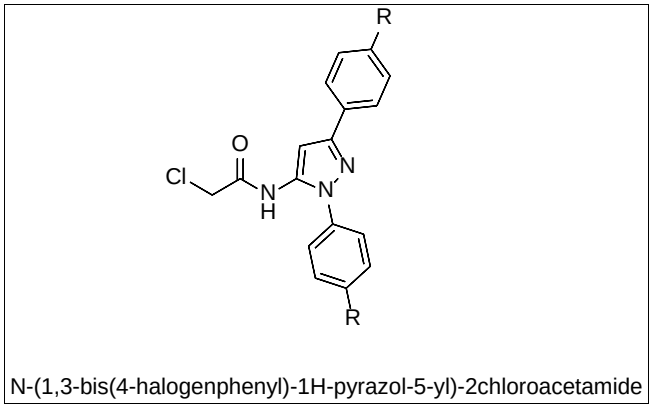

Fig 3: General structure of compound (IVa-c) and its derivatives

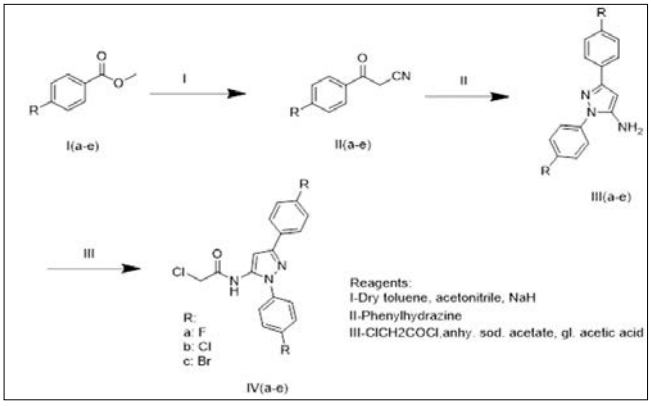

Scheme 1: Synthesis of thiourea derivatives

The novel derivatives of thiourea filtered as solid product with different melting point and different characteristic as below (Table 1).

Table 1: Physical properties of compound (IV) and its derivatives

Comp. derivatives	IUPAC name	M. P. (ºC)	Yield (%)	Appearance
Iva	N-(1,3-bis(4-fluorophenyl)-1H-pyrazol-5-yl)-2-chloroacetamide	(218-222) °C	81	Reddish
IVb	N-(1,3-bis(4-chlorophenyl)-1H-pyrazol-5-yl)-2-chloroacetamide	(230-235) °C	82	Light reddish
IVc	N-(1,3-bis(4-bromophenyl)-1H-pyrazol-5-yl)-2-chloroacetamide	(245-249) °C	79	Reddish to brown

Result and Discussion

1. In Silico ADME and Drug-Likeness Evaluation

Pharmacokinetic properties, drug-likeness and medicinal chemistry parameters of the synthesized compounds were predicted using SwissADME web, a freely available platform that is widely used in early drug discovery studies. This website allows the evaluation of absorption, distribution, metabolism and excretion (ADME) properties to find new compounds with suitable pharmacokinetic profiles and remove candidates that have a poor oral bioavailability or undesirable physicochemical characteristics. The evaluation of drug-likeness was established on Lipinski's Rule of Five, which is an important criterion in predicting the oral activity of drug candidates. This rule states that compounds have a higher adequate oral bioavailability when they have a MW molecular weight (MW)<500 g/mol, hydrogen-bond donors (HBD)≤5, hydrogen-bond acceptors (HBA)≤10 and calculated partition coefficient Log P<5. Also the number of rotatable bonds (NRB) and topological polar surface area (TPSA) are significantly influence factors for membrane permeability and oral absorption. Compounds with TPSA <140 Å² are deemed to possess desirable bioavailability [21]. The SwissADME Analysis showed that all synthesized derivatives exhibited moderate lipophilicity, which is a good property for orally active drugs. In addition, all compounds were compliant with Lipinski's rule of five without violation. Furthermore, based on their physicochemical properties, the derivatives were estimated to show high gastrointestinal absorption, acceptable aqueous solubility and limited blood–brain barrier (BBB) permeability indicating good pharmacokinetic characteristics making them more amenable for further drug development studies.

Table 2. Properties for studied compounds according to Swiss ADME

Property	IVa	IVb	IVc
Molecular Weight	347	379	466.9
Num. Rotatable Bonds	5	5	5
Num. H-bond Acceptors	4	4	4
Num. H-bond donr	1	1	1
Water Solubility Class	Soluble	Soluble	Soluble
Absorption in GI	Excellent	Excellent	Excellent
Permeant to BBB	Not pass	Not pass	Not pass
Lipinski Rule Violations	0	0	0

2. FT-IR of pyrazole Derivatives

The FT-IR spectrum of N-(1,3-bis(4-fluorophenyl)-1H-pyrazol-5-yl)-2-chloroacetamide (Fig. 4), showed characteristic absorption bands consistent with the proposed structure. A broad band at 3248 cm⁻¹ was assigned to (N–H) stretching vibrations of the amide and pyrazole NH groups, indicating intermolecular hydrogen bonding. The band at 2927 cm⁻¹ corresponded to aliphatic (C–H) stretching of the methylene group. A strong absorption at 1682 cm⁻¹ confirmed the amide carbonyl (C=O) group, while the bands at 1601 and 1494 cm⁻¹ were attributed to aromatic (C=C) stretching vibrations. The peaks at 1299 and 1233 cm⁻¹ were assigned to (C–N) and (C–F) stretching vibrations, respectively. Additional bands at 1045 and 970 cm⁻¹ corresponded to aromatic (C–H) bending and pyrazole ring vibrations, whereas the bands at 766 and 695 cm⁻¹ were characteristic of para-substituted benzene rings. Overall, the observed FT-IR data confirmed the successful synthesis of the target compound and were in good agreement with the proposed molecular structure [26].

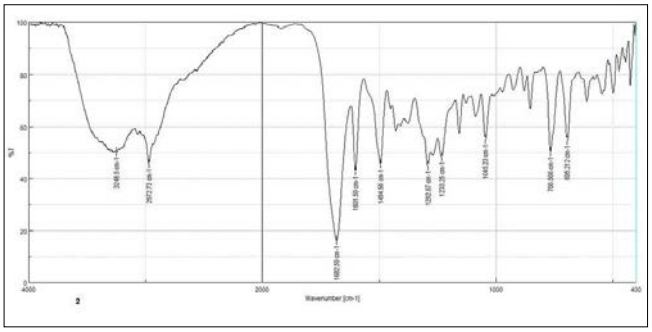

Fig 4: FT-IR spectrum of N-(1,3-bis(4-fluorophenyl)-1H-pyrazol-5-yl)-2-chloroacetamide (IVa)

The FT-IR spectrum of N-(1,3-bis(4-chlorophenyl)-1H-pyrazol-5-yl)-2-chloroacetamide (Fig. 5), exhibited characteristic absorption bands consistent with the proposed structure. A broad band at 3209 cm⁻¹ was assigned to (N–H) stretching vibrations of the amide and pyrazole NH groups, indicating hydrogen-bonding interactions. The bands at 2924 and 2848 cm⁻¹ corresponded to aliphatic (C–H) stretching of the methylene group. A strong absorption at 1679 cm⁻¹ confirmed the amide carbonyl (C=O) group, while the peaks at 1597 and 1495 cm⁻¹ were attributed to aromatic (C=C) stretching vibrations. The band at 1281 cm⁻¹ was assigned to (C–N) stretching, and the absorption at 1009 cm⁻¹ corresponded to aromatic (C–H) bending and pyrazole ring vibrations. The bands at 754 and 693 cm⁻¹ confirmed the presence of para-substituted benzene rings, whereas the weak band at 404 cm⁻¹ was attributed to (C–Cl) stretching. Overall, the FT-IR data confirmed the successful synthesis of the target compound and were consistent with the proposed molecular structure [26].

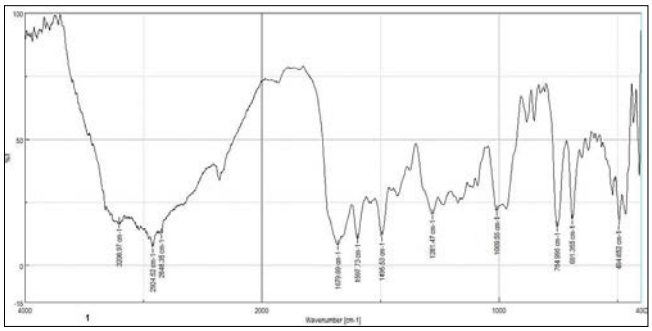

Fig 5: FT-IR spectrum of N-(1,3-bis(4-chlorophenyl)-1H-pyrazol-5-yl)-2-chloroacetamide (IVb)

The FT-IR spectrum of N-(1,3-bis(4-bromophenyl)-1H-pyrazol-5-yl)-2-chloroacetamide (Fig. 6), exhibited characteristic absorption bands consistent with the proposed structure. A band at 3252 cm^{-1} was assigned to (N–H) stretching vibrations of the amide and pyrazole NH groups. The bands at 3006 cm^{-1} and 2929–2854 cm^{-1} corresponded to aromatic and aliphatic (C–H) stretching vibrations, respectively. A strong absorption at 1674 cm^{-1} confirmed the amide carbonyl (C=O) group, while the bands at 1587 and 1490 cm^{-1} were attributed to aromatic (C=C) stretching. The peaks at 1388 and 1265 cm^{-1} were assigned to (C–N) stretching vibrations, and the region 1170–1067 cm^{-1} was associated with pyrazole ring vibrations. The band at 970 cm^{-1} corresponded to aromatic (C–H) bending, whereas the bands at 845 and 806 cm^{-1} confirmed the presence of para-substituted benzene rings. Finally, the bands at 617, 538, and 503 cm^{-1} were attributed to (C–Br) stretching vibrations, providing evidence for the bromine substituents, while (C–Cl) stretching may contribute in the lower-frequency region. Overall, the FT-IR data confirmed the successful synthesis of the target compound and agreed well with the proposed molecular structure [26].

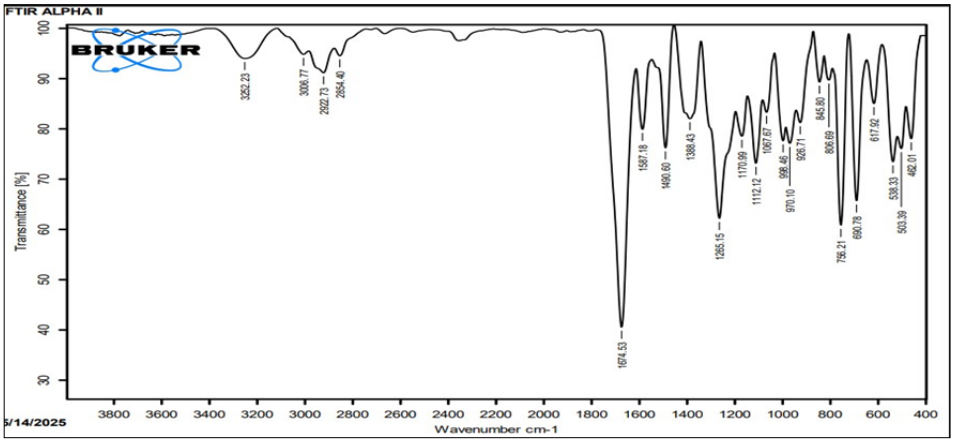

Fig 6: FT-IR spectrum of N-(1,3-bis(4-bromophenyl)-1H-pyrazol-5-yl)-2-chloroacetamide (IVc)

Table 3: IR Spectroscopy for pyrazole derivatives

Functional Group	Iva	IVb	IVc
(N–H) Stretch	3248	3209	3252
(C– H) Aromatic /Aliphatic	2927	2924, 2848	3006, 2929, 2854
(C=O) (Amide)	1682	1679	1674
(C–N) (Amide/ Pyrazole)	1299,1233	1281	1265
(C=C) Aromatic	1601,1494	1597 / 1495	1587, 1490
(C– H) Aromatic	766,695	754, 693	845, 806
(C–X) Stretch (X=F,Cl,Br,I)	1233 (C–F)	693 (C–Cl)	617, 538, 503 (C–Br)
CH_2–Cl Stretch	1045	1009	1067

3. Mass spectra of derivatives

Table 4: Mass Spectroscopy for pyrazole derivatives

Compound	Exact M.W	M.+ (m/z)
IVa	347	347.2
IVb	379	380.3
IVc	466.9	466.3

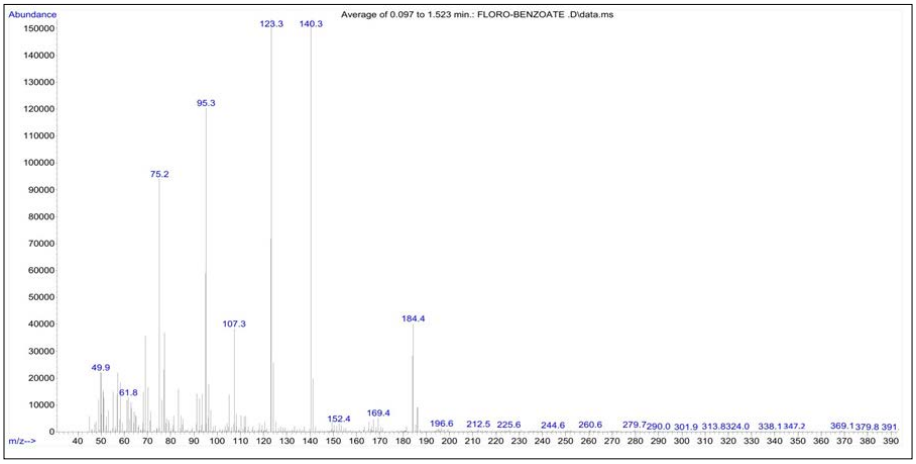

Fig 7: Mass Spectra of IVa

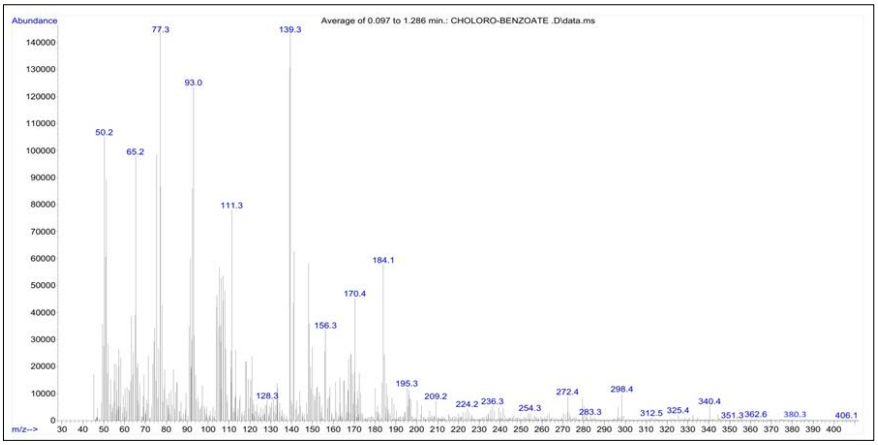

Fig 8: Mass Spectra of IVb

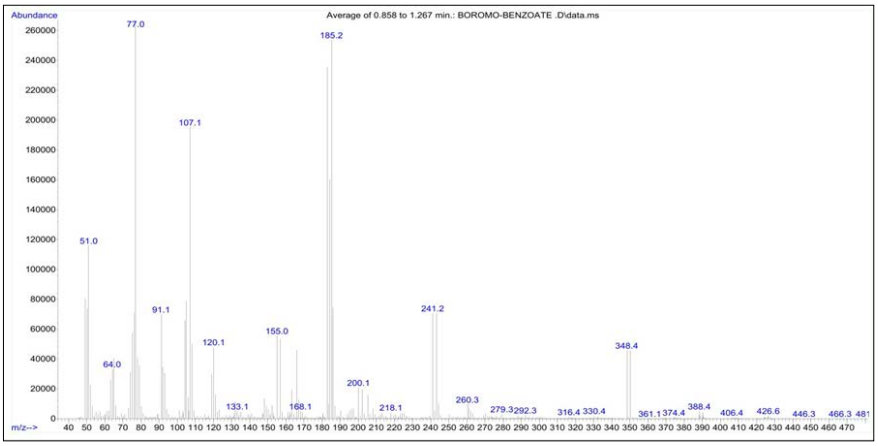

Fig 9: Mass Spectra of IVc

4. ^{1}H-NMR Spectra of Synthesized Compounds.

N-(1,3-bis(4-fluorophenyl)-1H-pyrazol-5-yl)-2-chloroacetamide (IVa).

^{1}H-NMR (400 MHz, DMSO) δ 11.60 (s, 1H, (–NH–C(=O)–)), 8.02 (dd, *J* = 9.0, 5.6 Hz, 1H , Ar-H) , 8.01 (dd, *J* = 9.0, 5.6 Hz, 1H , Ar-H), 8.00 (dd, *J* = 9.0, 5.6 Hz, 1H , Ar-H), 7.98 (dd, *J* = 9.0, 5.6 Hz, 1H , Ar-H), 7.42 (s, 1H , (s, Pyrazole H (1H))), 7.34 (t, *J* = 8.9 Hz, 1H , Ar-H) , 7.32 (t, *J* = 8.9 Hz, 1H , Ar-H), 7.29 (t, *J* = 8.9 Hz, 1H , Ar-H) , 4.27 (s, 2H, CH_2–Cl) .

N-(1,3-bis(4-chlorophenyl)-1H-pyrazol-5-yl)-2-chloroacetamide (IVb).

^{1}H-NMR (400 MHz, DMSO) δ 10.36 (s, 1H, (–NH–C(=O)–)) , 7.96 (d, *J* = 1.8 Hz, 1H , Ar-H) , 7.96 (d, *J* = 1.8 Hz, 1H , Ar-H) , 7.59 (d, *J* = 3.8 Hz, 1H , Ar-H), 7.58 (d, *J* = 3.8 Hz, 1H , Ar-H) , 7.31 (d, *J* = 16.0 Hz, 1H , Ar-H) , 7.27 (d, *J* = 16.0 Hz, 1H , Ar-H), 7.17 (s, 1H , (s, Pyrazole H (1H)), 4.29 (s, 2H, CH_2–Cl) .

N-(1,3-bis(4-bromophenyl)-1H-pyrazol-5-yl)-2chloroacetamide (IVc).

^{1}H-NMR (400 MHz, DMSO) δ 11.54 (s, 1H , (–NH–C(=O)–)), 7.97 (d, *J* = 8.5 Hz, 2H , Ar-H), 7.87 (d, *J* = 8.5 Hz, 2H , Ar-H), 7.79 (d, *J* = 8.5 Hz, 2H , Ar-H), 7.71 (d, *J* = 8.5 Hz, 2H , Ar-H), 7.43 (s, 1H , H Pyrazole H), 4.27 (s, 2H , CH_2–Cl).

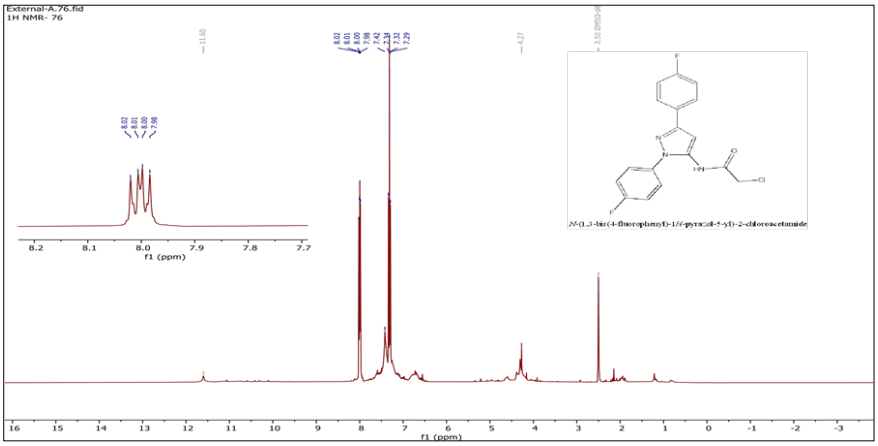

Fig 10: ^{1}H-NMR N-(1,3-bis(4-fluorophenyl)-1H-pyrazol-5-yl)-2-chloroacetamide (IVa)

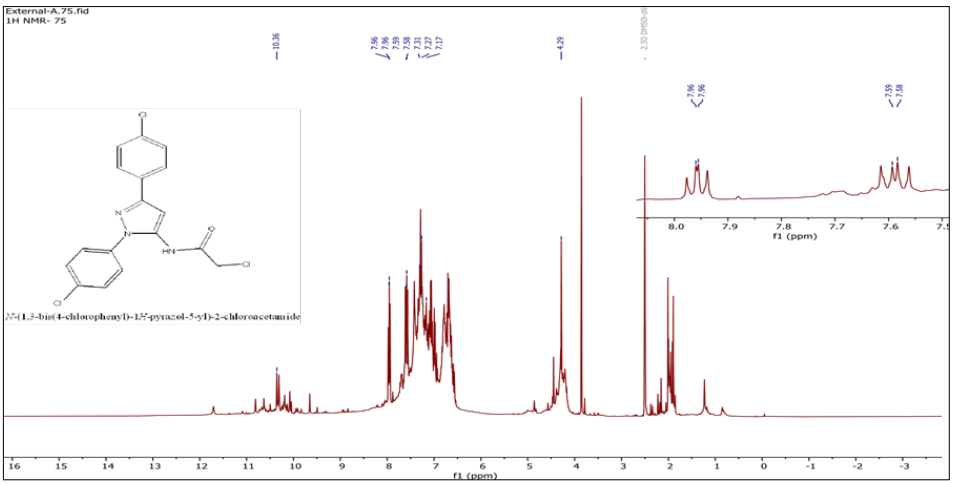

Fig 11: [1]H-NMR N-(1,3-bis(4-chlorophenyl)-1H-pyrazol-5-yl)-2-chloroacetamide (IVb)

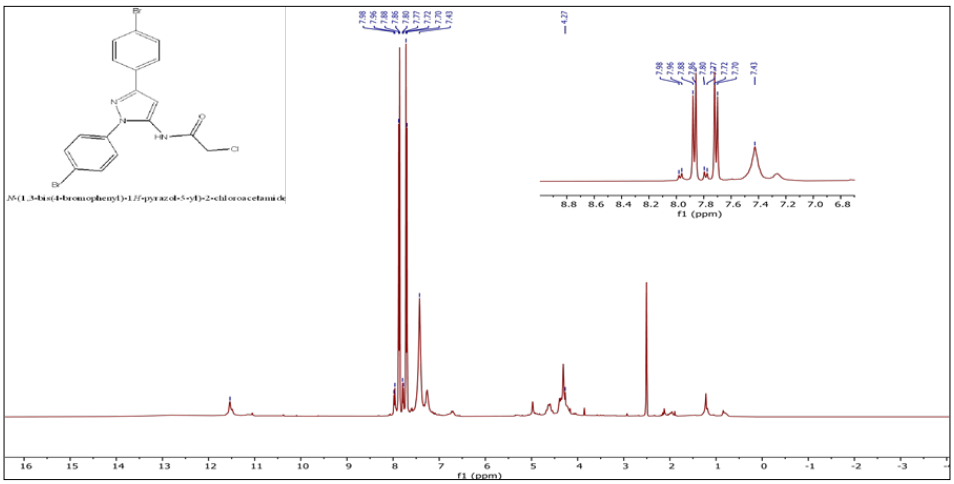

Fig 12: [1]H-NMR N-(1,3-bis(4-bromophenyl)-1H-pyrazol-5-yl)-2-chloroacetamide (IVc)

5. Biological evaluation Cytotoxicity against MCF-7

Compounds IVa–IVc were evaluated for their cytotoxic activity against MCF-7 breast cancer cell line. Results showed that some of the derivatives had significant cytotoxic activity. Of these, IVa and IVb had the lowest values of IC_{50}, showing potential anticancer activity and suggesting a basis for continued study. Conversely, compounds IVc were cytotoxic. The implications of these observations are that structural modifications, specifically at the benzamide moiety with regards to both substitution type and position/depth, do dictate varying levels of inhibition potency against the enzyme as well as cytotoxicity. The anticancer activity of the prepared pyrazole–thiourea derivatives (IVa–IVc), presented in (Table 5), displayed valuable and encouraging information for future designs as potential candidates for anticancer drug development.

Table 5: Cytotoxicity of synthesized compounds against MCF at 500 (µM).

I.D	MCF7 IC_{50} (µM)	MCF-7 Inhibition (%)
IVa	75.34	73.24
IVb	167.45	66.55
IVc	238.21	58.24
Rescovitine	20.31	97.33

The IC_{50} results clearly demonstrate that CDK-2 inhibitory activity is influenced by both the electronic properties and steric characteristics of the para substituents on the aromatic rings, which is consistent with the behavior of cyclin dependent kinase inhibitors targeting the ATP-binding site [27]. Among the synthesized compounds, the IVa derivative (IC_{50} = 1.77 µM) exhibited the highest activity as shown in (Table 5), suggesting that small electron-withdrawing substituents enhance binding affinity while minimizing steric hindrance within the active site. This can be attributed to the ability of fluorine to modulate electronic distribution and improve molecular interactions without significantly increasing molecular size [28].

The IVb derivative (IC_{50} = 2.11 µM) showed slightly lower activity as shown in (Table 5), despite its electron-withdrawing nature, which may be explained by its larger atomic size affecting optimal binding orientation within the ATP-binding pocket. Similarly, the IVc derivative (IC_{50} = 4.97 µM) displayed reduced activity as shown in (Table 5), indicating that increasing steric bulk can negatively influence binding efficiency [29]. Overall, the observed activity trend (F > Cl > Br) indicates that both electronic and steric factors play a crucial role in determining inhibitory potency. While electron-withdrawing groups improve interaction with the enzyme, steric effects govern the ability of the compound to adopt a favorable conformation within the binding pocket. When compared with the reference inhibitor roscovitine (IC_{50}= 0.61 µM), the synthesized compounds exhibit a clear structure–activity

relationship, confirming that careful optimization of substituent size and electronic properties is essential for improving CDK-2 inhibitory activity[29].

Conclusion

The results showed that IVa and IVb were the most potent cytotoxic agents against MCF-7 breast cancers with effects similar to rescovitine. The assorted biological activity among the synthetic derivatives reflects that the nature of the substituents on the benzamide ring is key to inhibition. IVa & IVb exhibited potent anti-cancer activity, and IVc. Structure activity relationship (SAR) analyses suggested that electron withdrawing groups increased the affinity towards target binding and biological activity, such as the fluorine substituent, although bulkier steric substituents tended to exhibit a reduced potency. In addition, the ADMET evaluation indicated acceptable pharmacokinetic properties for all compounds synthesized in this study, including good aqueous solubility, appropriate gastrointestinal absorption and compliance with Lipinski's rule of five supporting their potential oral bioavailability as a drug candidate. IVa–IVc combinations of these pyrazole–thiourea derivatives exhibited excellent anticancer activity, and among them IVa and IVb could be recognized as interesting lead compounds for further development toward selective CDK2 inhibitors with beneficial pharmacokinetic profile.

References

1. Hanahan D, Weinberg RA. The Hallmarks of Cancer. Cell,2000:100(1):57–70.
2. Vogelstein B, Papadopoulos N, Velculescu VE, Kinzler KW, Zhou S, Diaz LA. Cancer Genome Landscapes. Science,2013:339(6127):1546–1558.
3. Sung H, Ferlay J, Siegel RL, *et al*. Global Cancer Statistics 2020: GLOBOCAN Estimates of Incidence and Mortality Worldwide for 36 Cancers in 185 Countries. CA Cancer J Clin,2021:71(3):209–249.
4. Awad KT, Al-Salman HNK, Najm MAA. Synthesis and CDK2 inhibition profiling of novel pyrazolyl-thiourea derivatives as potential anti-inflammatory agents. Anaesth Pain Intensive Care,2025:29(6):594–599.
5. Islami F, Goding Sauer A, Miller KD, *et al*. Proportion and number of cancer cases and deaths attributable to potentially modifiable risk factors in the United States. CA Cancer J Clin,2018:68(1):31–54.
6. Plummer M, de Martel C, Vignat J, Ferlay J, Bray F, Franceschi S. Global burden of cancers attributable to infections in 2012: a synthetic analysis. Lancet Glob Health,2016:4(9):e609–e616.
7. Liang D, Yan Y, Bai S, *et al*. The impact of high-risk cytogenetic abnormalities in extramedullary multiple myeloma in the era of novel agents: insights from a multicenter study. BMC Cancer, 2024, 24, 1551.
8. Chen S, Cao Z, Prettner K, *et al*. Estimates and Projections of the Global Economic Cost of 29 Cancers in 204 Countries and Territories From 2020 to 2050. JAMA Oncol,2023:9(4):465–474.
9. Schuster C, Gabel A, Drost HG, *et al*. Evolutionary transcriptomics unveils rapid changes of gene expression patterns in flowering plants. Cell,2026:189(2):375–385.e14.
10. Loeb S, Langford AT, Bragg MA, Sherman R, Chan JM. Cancer misinformation on social media. CA Cancer J Clin,2024:74(5):453–464.
11. Bray F, Laversanne M, Weiderpass E, Soerjomataram I. The ever-increasing importance of cancer as a leading cause of premature death worldwide. Cancer,2021:127(16):3029–3030.
12. GBD 2019 Cancer Risk Factors Collaborators. The global burden of cancer attributable to risk factors, 2010–19: a systematic analysis for the Global Burden of Disease Study 2019. Lancet,2022:400(10352):563–591.
13. Farmer P, Frenk J, Knaul FM, *et al*. Expansion of cancer care and control in countries of low and middle income: a call to action. Lancet,2010:376(9747):1186–1193.
14. Wen S, Arakawa H, Tamai I. Uric acid in health and disease: From physiological functions to pathogenic mechanisms. Pharmacol Ther, 2025.
15. Li W, Hao J, Cai L, *et al*. Biomaterial-minimalistic photoactivated bioprinting of cell-dense tissues. Cell,2026:189(1):106–122.26.
16. Pu CY, Lusk CM, Neslund-Dudas C, Gadgeel S, Soubani AO, Schwartz AG. Comparison between the 2021 USPSTF Lung Cancer Screening Criteria and Other Lung Cancer Screening Criteria for Racial Disparity in Eligibility. JAMA Oncol,2022:8(3):374–382.
17. Bray F, Laversanne M, Sung H, *et al*. Global Cancer Statistics 2022: GLOBOCAN estimates of incidence and mortality worldwide. CA Cancer J Clin, 2024.
18. Groeneveld CS, Fontugne J, Cabel L, *et al*. Tertiary lymphoid structures marker CXCL13 is associated with better survival for patients with advanced-stage bladder cancer treated with immunotherapy. Eur J Cancer, 2021, 148, 181–189.
19. Molero A, Hernandez S, Alonso M, *et al*. Assessment of PD-L1 expression and tumour infiltrating lymphocytes in early-stage non-small cell lung carcinoma with artificial intelligence algorithms. J Clin Pathol,2025:78(7):456–464.
20. Vázquez-Villa H, Rueda-Zubiaurre A, Fernández D, *et al*. Chemical probes for the identification of the molecular targets of honokiol. Eur J Med Chem, 2025, 283, 117102.
21. Tran KB, Lang JJ, Compton K, *et al*. The global burden of cancer attributable to risk factors, 2010–19: a systematic analysis for the Global Burden of Disease Study 2019. Lancet,2022:400(10352):563–591.
22. Al-Halbosy ATF, *et al*. Thiourea Derivative Metal Complexes: Spectroscopic, Anti-Microbial Evaluation, ADMET, Toxicity, and Molecular Docking Studies. Inorganics, 2023, 11.
23. Drauz K, Kleemann A, Wolf-Heuss E. Process for the production of 3-oxonitriles. US Patent US4728743A, 1988.
24. Wei Y, Liu P, Liu Y, *et al*. NIS-promoted three-component reaction of 3-oxo-3-arylpropanenitriles with arylsulfonyl hydrazides. Org Biomol Chem,2021:19(17):3932–3939.
25. Kendre BV, Landge MG, Bhusare SR. Synthesis and biological evaluation of some novel chloroacetamide derivatives containing pyrazole nucleus. Bioorg Med Chem Lett,2014:24(15):3670–3674.

26. Silverstein RM, Webster FX, Kiemle DJ, Bryce DL. Spectrometric Identification of Organic Compounds. 9th ed. Hoboken, NJ: John Wiley & Sons, 2025.
27. Asghar U, Witkiewicz AK, Turner NC, Knudsen ES. The history and future of targeting cyclin-dependent kinases in cancer therapy. Nat Rev Drug Discov,2015:14(2):130–146.
28. Purser S, Moore PR, Swallow S, Gouverneur V. Fluorine in medicinal chemistry. Chem Soc Rev,2008:37(2):320–330.
29. Tadesse S, Caldon EC, Tilley W, Wang S. Cyclin-dependent kinase 2 inhibitors in cancer therapy: an update. J Med Chem,2019:62(9):4233–4251.